

Thermography Studies and Electric Measurement of Partial Discharges in Underground Power Installations

A. González-Parada, E. Camacho-Lespron, R. Guzmán-Cabrera, J. Rosales García

Electrical Department, Engineering Division,
University of Guanajuato

Abstract.- The principal damage on underground power cables installations is due to Partial Discharge (PD) activity.

A comparative study between the electrical measurements of onset PD and thermography images is presented. The study was carried out with specific faults in the installation of accessories, their evolution being monitored by inductive electric sensors and correlating the results with thermography images taken during test development.

The thermo graphic image analysis is made by digital image processing algorithm. An approach is proposed to effectively analyze digital, based on texture segmentation for the detection of early failure stage. The proposed algorithm was tested and compare with the measurements obtained from electrical sensor in the failure point. The result was found to be suitable to distinguish onset failures from the background tissue using morphological operators and the extract them through machine learning techniques and a clustering algorithm for intensity-based segmentation.

Keywords— Failure onset, partial discharges, power cables, thermography, texture segmentation.

1. INTRODUCTION

During ageing of a defect in an underground power cables, different PD mechanisms can occur. Aged defects have lower generally inception voltage than small defects. PDs are measured by charge displacement in the cable to the defect, there

is related to the energy dissipated during a discharge and the volume of the cavity [1,2,3].

In the market exists several systems of different manufacturers to measure PD; the technical difference between systems are basically in the difference of the energizing source [4,5].

In this work a novel approach for failure detection on underground power cables is presented. The proposed method allows us to detect the thermal effect of PD by digitally processing of thermal images of the electrical installation of cable accessories. The image processing consists mainly of an intensity-based texture segmentation algorithm that allows identifying and extracting the regions of the thermography picture where the failure occurs by using morphological operators and machine learning techniques, respectively. This approach offers the capability to operate in an incipient failure detection scheme, i.e. the failure detection process is carried out without shutting the system down [5], by taking advantage of the architectural distortion (alterations in density, shape, and margins) produced by variations in the temperature distribution to effectively segment and extract the regions of interest.

2. THEORETICAL BACKGROUND

2.1 Partial Discharge process.

PD is in general consequence of the local electric stress concentrations in the insulation or on the surface of the insulation. Generally appears as pulse, having duration of much less than $1 \mu\text{s}$ and usually accompanied by emission of sound, light, heat, and chemical reactions. The PD type depend of the defect localisation and it could be internal or in the surface. The figure 1 shows the electrical model for a) PD on internal defect insulation and b) PD on the insulation surface [6].

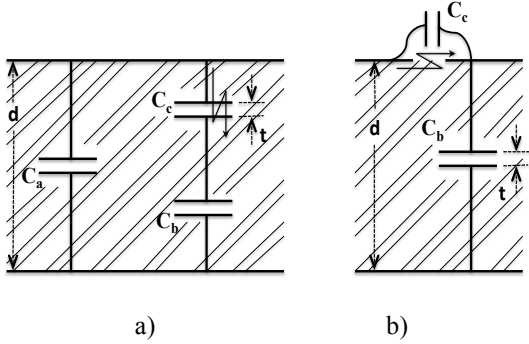


Fig. 1 Electrical representation of a) internal partial discharges and b) superficial partial discharges

Considering that the gas-filled cavity breakdown stress is E_c , and treating the cavity as series capacitance with the dielectric without cavity in the dielectric (see figure 2) [7], the capacitance can be write as:

$$C_b = \frac{\epsilon_0 \epsilon_r A}{d - t} \quad (1)$$

$$C_c = \frac{\epsilon_0 A}{t} \quad (2)$$

The voltage across the cavity is:

$$U = \frac{C_b}{C_c + C_b} \Delta V = \frac{\Delta V}{1 + \frac{1}{\epsilon_r} \left(\frac{d}{t} - 1 \right)} \quad (3)$$

Therefore the voltage across the dielectric that will initiate the discharge in the cavity will be given by:

$$V_i = E_c \left[1 + \frac{1}{\epsilon_r} \left(\frac{d}{t} - 1 \right) \right] \quad (4)$$

When a PD occurs, some charge is displaced from C_c to C_b , as follow: the voltage across C_c drops to ΔV ; due that the voltage across C_b increases with ΔV , then the voltage over C_c becomes V , and the charge displacement to C_b is given by $q = C_b \Delta V$.

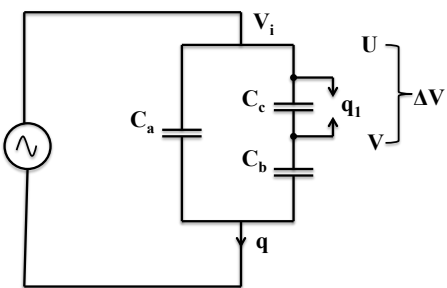


Fig. 2 PD electrical model

The energy dissipated during a discharge can be related to the charge according as follow; before

discharge, the energy stored in C_c is:

$$W_{C_c} = \frac{1}{2} C_c U^2 \quad (5)$$

after discharge, the energy stored in C_c is:

$$W_{C_c} = \frac{1}{2} C_c V^2 \quad (6)$$

The total dissipated energy in the cavity becomes:

$$W_t = \frac{1}{2} C_c (U^2 - V^2) = \frac{1}{2} C_c \Delta V (U + V) \quad (7)$$

Usually $C_b \ll C_c$, then the dissipated energy becomes:

$$W_t \approx \frac{1}{2} C_b \Delta V \cdot V_i = \frac{1}{2} q V_i \quad (8)$$

This energy is dissipated as heat, and can be detected in the previous moments to the failure by a thermography camera. In the case of an incipient failure, the energy released is not sufficiently large so that the temperature rise cannot be detected by a thermal imaging camera. Therefore, variations in the texture of the image could be done by means of a digital process of images.

2.1 Image process methodology

The proposed technique is based on feature extraction through texture analysis for the identification and discrimination of suspicious areas related to the failure. As texture-based analysis methods characterize texture in terms of the extracted feature, segmentation depends not only on the images under study but also on the aim for which the image texture is used [12].

A general flow diagram of the proposed image processing is shown in Figure 3. In general, the process begins with an input thermal image that is to be processed in different stages until an output image containing the regions of interest, and thus the possible system failures, is generated.

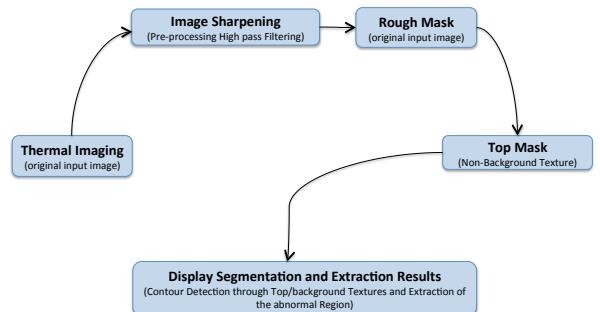


Fig. 3 Flow diagram of the intensity-based texture segmentation algorithm.

As shown in Figure 3, the regions of interest are identified and then extracted using the background

texture as a contrast mask against the original input image. This means that the regions identified as part of the object texture are defined directly by the background regions in the rough mask.

Figure 4 shows a more detailed view of the sub-stages internally involved in the segmentation and extraction. These sub-stages are described in detail below; according to the properties of the transition regions exhibited by the thermographic images, gradient-based algorithms are to be discarded and entropy-based texture segmentation is desired instead since it offers a significantly more efficient performance in the case when a large variety of changes in the gray scale occurs in a single transition region, i.e. fuzzy and not well defined transition regions [13].

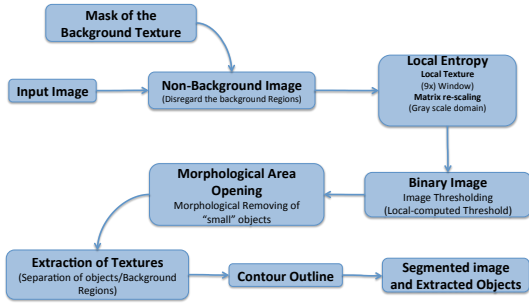


Fig. 4 Internal structure of the stage where the object’s texture is extracted.

The definition of entropy proposed by Pun [14] is a statistical measure of randomness; IT was based on Shannon’s theory of communication and considers the operation over the full image. In this case, the same concept is scaled down to a small region Ω_k of size $(M_k \times N_k)$ within the image such that the local entropy is defined for this window as follows:

$$E(\Omega_k) = - \sum_{i=0}^{L-1} P_i \log(P_i) \quad (9)$$

where

$$P_i = \frac{n_i}{(M_k \times N_k)} \quad (10)$$

Additional information can be obtained from higher order histograms and entropies of new images generated based on the properties of the original input image [15]. The proposed algorithm considers only the first-order entropy, which makes it easy to implement and computationally cost effective.

As shown in Figure 4, the definition of the background texture starts with the calculation of the local entropy of the image using Eqs. (9)–(10). This stage has two inputs: the high-pass filtered image (i.e. pre-processed image) and the threshold gray

level. The first-order process described above is implemented in the pre-processed image using a window size of 9×9 pixels and considering only the adjacent (surrounding) neighbors of the current pixel considered in the calculation of the local entropy. The entropy image is then binarized via simple thresholding such that a primitive (binary, black and white) version of the background texture mask is available right after this stage.

However, this binary image containing the background texture is not considered for used for further processing and it needs to be cleaned first. The “small” objects are removed from this image using the “area opening operation” method; this stage receives a reference area as input parameter.

In order to introduce the less shape defects and obtain the transition regions accurately; an edge smoothing is performed on the area-opened image, applying a sequential process of dilation followed by erosion using a square mask of dimensions 9×9 pixels. Filling the holes within the background texture connects the isolated background pixels. Once this process has completed, a binary image containing the background texture mask is available for further stages.

The next step, in which the object texture is identified, has two inputs: the original (gray scale) input image and the (binary) image of the background mask obtained in the previous stage. The background binary mask is used to isolate the “non-background” region from the input image. Texture analysis is performed over the “non-background” region by computing the local entropy similarly to the first stage of the process. The disregarded region of the original image (background mask) does not contribute to further results due that the local entropy is minimal for regions consisting of pixels with the same gray value [16]. The resulted binary image contains a preliminary version of the top (object) texture.

Finally, both area opening and edge smoothing is performed on the top texture image with parameters to those used previously. Once the binary image containing the top texture is ready, it can be readily used to extract the regions of interest from the original image.

3. EXPERIMENTAL AND TESTS RESULTS

In order to validate this image analysis process, a laboratory test was performed considering the induced failure in terminals. A photograph of the experimental test setup is illustrated in Figure 5. A power transformer is used to simulate high voltage applied in the transmission line and the charge is induced in the line by a current transformer.

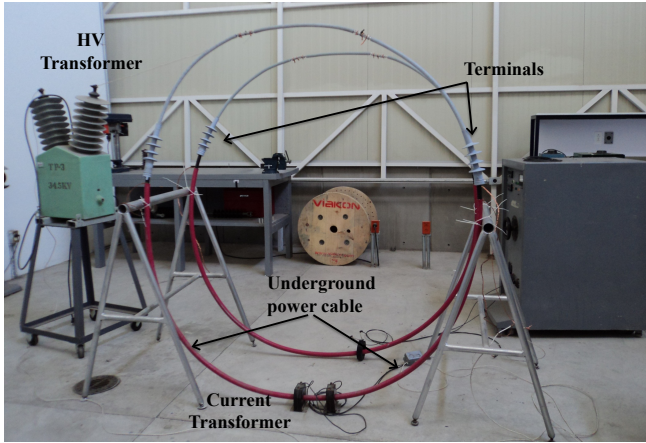


Fig. 5 General Test setup for electrical PD detection on underground power cable model.

During the test, a commercial 1/0 AWG cable with 100 % XLP insulation and wire screen was used. The voltage between the phase and ground terminals is set to 15 kV and a current of 60 A circulate in the system considering a real charge of the line. Commercial 15 kV silicon terminals was used, in this case it was an Elastimold model PCT1 silicon terminals for 1/0 AWG power cables.

A failure is induced in the terminal having a small separation of the terminal stress cone and the outer semiconductive layer. This separation induces superficial PD in the terminal causing a temperature increment by the charge transference and electrical activity. As show in eq. 8, the total energy dissipated depends unique of the initial voltage of discharge and not of the current circulating on the cable. Figure 6, shows a picture of the failure induced in the terminal where the separation stress cone of the terminal and the cable outer semiconductive layer can be clearly appreciated.

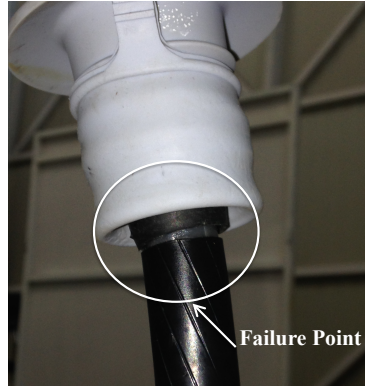


Fig. 6 Terminal with failure induced in the cable with the stress cone separated of the outer semiconductive screen.

In order to measure the failure electrical signal, the system was instrumented with a Rogowski coil constructed specially for the test; it was connected

to a standard digital oscilloscope FLUKE 190-102, that allows continuously monitoring of the circulating current cable. With this system the onset PD can be register in order to assure the occurrence of the failure. Figure 7 shows the sensor position in the terminal.



Fig. 7 Position of the sensor in the terminal to check the PD activity in cable.

PD activity was verified in both terminals by means of sensors fixed as shown in figure 7; the signal obtained was plotted to see the difference between the terminal with defect and the terminal without failure. Figure 8 shows the PD present in the terminal whit failure, the absence being noticed in the terminal in good condition

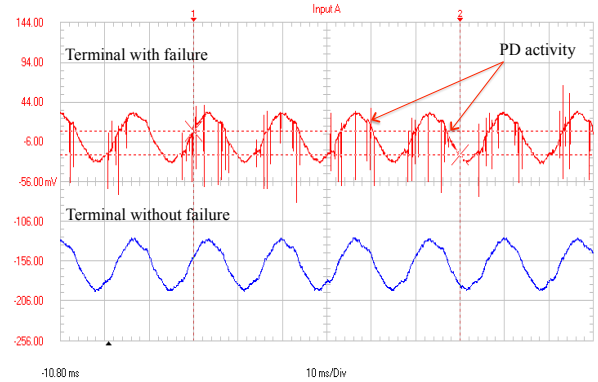
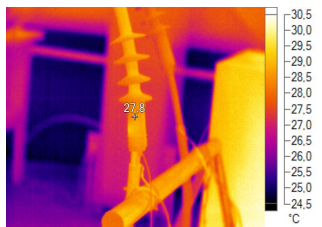


Fig. 8 PD signal activity obtained from terminal with failure (upper) and terminal in good condition (lower).

Figures 9 and 10 shows the pictures of the terminals with failure and without failure, these picture were taken with thermography camera FLUKE Ti 132 under infrared palettes and white-light, respectively. The temperature scale shown in the infrared image is the actual temperature measured using the camera calibration such that the temperature distribution over the pictures is provided.



a)



b)

Fig. 9 Pictures of the terminal with failure and partial discharges in two different color palettes. a) White light and b) infrared

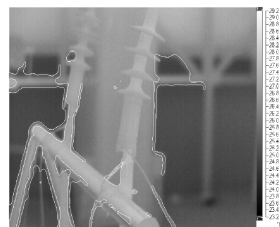
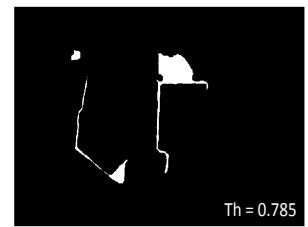
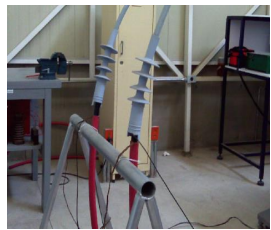
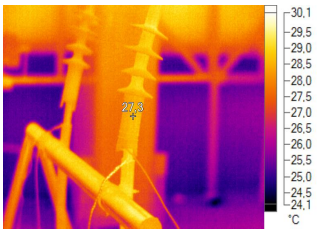
 $Th = 0.785$ 

Fig. 12 Segmentation and extraction of the terminal in good condition without failure point.



a)



b)

Fig. 10 Pictures of the terminal in good condition in two different color palettes. a) White light and b) infrared

Despite an accurate contactless temperature measurement can be achieved with a good calibration of the infrared camera, the proposed image processing never sees this calibration but only the textures defined by the gray levels that naturally arise due to thermal effects.

In order to orientate the analysis of the thermal effects to the region of interest, infrared images of the experimental setup where processed digitally using segmentation and extraction algorithms based on the texture and morphological image analysis described above.

Figure 11 and 12 shows the result of a processed picture of the experimental setup after segmentation and extraction, respectively. It can be clearly seen that the region of point of failure can be successfully identified.

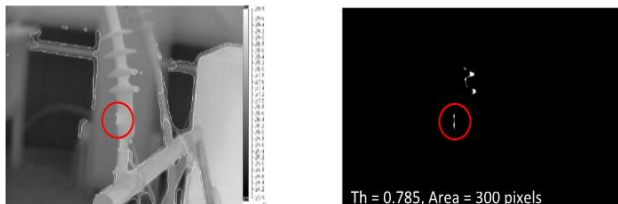


Fig. 11 Segmentation and extraction of the point of failure in terminal with failure.

The proposed instrumentation allows not only calibrated measures of the temperature over several regions of the experimental setup but also validate the physical location of the failure obtained from the image process.

Moreover, since the digital processing is to operate on infrared images obtained from contactless instrumentation, the proposed approach provides a suitable and powerful tool for safe, continuous, and effective failure detection that allows remote control and uninterrupted *in situ* measurement in which disconnection line is not required.

4. CONCLUSIONS

The proposed monitoring method and analysis system test set up allows inducing a variety of controlled failures in order to accurately characterize the electrical behavior of the partial discharges phenomenon. This detailed characterization can lead to diagnose and prevent a variety of failures in further applications.

The location where the induced failure occurs is confirmed by the processing of infrared images based on texture segmentation and morphological extraction algorithms thus allowing relate changes in the electrical behavior only to the induced failure, resulting in reliable performance of the proposed measurement and analysis system.

5. REFERENCES

1. E. Gulski, et all, in *Cigre ELECTRA4*, pp 34-43 (2003).
2. G. Paoletti, A. Golubev, in *IEEE IAS Pulp and Paper Industry Conference* (2009).
3. M. Tozzi, in *University of Bologna Ph.D Thesis* (2010).
4. E. Lemke, et all, in *Electra 61*, No. 241, December (2008).
5. E. Lemke, et all, in *Electra 63* No. 226, june (2006).
6. R. Bartnikas, in *IEEE Transactions on Electrical Insulation*, vol 25 No. 1, pp 111-124, (1990).
7. R. Bartnikas, in *IEEE Transactions on Electrical Insulation*, vol. 9 No. 5, pp 763-808, (2002).
8. L.W. van Veen, in *Delft University of Technology M.Sc. Thesis* (2014).
9. P. Cichecki, E. Gulski, J.J. Smit, T. Hermans, R. Bodega, P.P. Seitz, in *IEEE Electrical Insulation Conference*, Montreal Ca, pp 5-9, (2009).
10. S.A. Boggs, G. C. Stone, in *IEEE Transactions on Electrical Insulation*, vol. EI-17, No. 2 (1982).

11. T. Serre, L. Wolf, S. Bileschi, M. Riesenhuber, and T. Poggio, in *IEEE Trans. on PAMI*, vol. 29, no. 3, (2007).
12. H.D. Cheng, X. Cai, X. Chen, L. Hu, X. Lou, in *Pattern Recognition*, 36, 2967 (2003).
13. R.C. Gonzalez, R.E. Woods, S.L. Eddins, in *Digital Image Processing Using MATLAB* (Pearson Prentice Hall, Upper Saddle River, NJ,) chap 11 (2003).
14. T. Pun, in *Signal Process*, 2, 223, (1980).
15. J.J. Gerbrands, in *Delft University of Technology*, PhD. Thesis (1998).
16. J. Yáñez, S. Muñoz and J. Montero: "Graph coloring inconsistencies in image segmentation." Computer Engineering and Information Sciences 1, 435-440 (2008).
17. C. Yan, N. Sang, T. Zhang, in *Pattern Recognition Letters*, 24, 2935 (2003).
18. Ch. Thum, in *Opt. Act Int. J. Opt.* 31, 203 (1984).
19. P. Soille, in *Morphological Image Analysis: Principles and Applications* (Springer, New York, pp164-165 (1999).
20. L. Vincent in *IEEE Transactions on Image Process*, 2, 176 (1993).
21. S.S. Basha, K.S. Prasad in *Int. J. Comput. Sci. Netw. Secur.* 8, 211 (2008).

6. AUTHORS



Adrián González-Parada.- Electrical engineering from the Queretaro Technological Institute, obtained a Masters degree in electrical engineering specializing in high voltage from DICIS, University of Guanajuato, Mexico and Phd in electrical engineering from the Polytechnic University of Catalonia in Barcelona, Spain. He is research-professor in the DICIS of the University of Guanajuato and responsible of the applied superconductivity and special electrical machines Laboratory. His areas of interest are applied superconductivity in electrical equipment, efficient use of energy in electrical power systems and electrical equipment reliability in the electrical grid.



Emiliano Camacho-Lespron, study Electrical Engineering, graduated in 2015 from Division of Engineering's Campus Irapuato-Salamanca, University of Guanajuato, he has worked with Superconductive Materials and High

Voltage projects and he has received several courses related to Electrical Machines, Energy Efficiency and Energy Saving, Thermography and he has worked in two Summers Research on issues related to Superconductivity.



Rafael Guzmán-Cabrera.- Full time Professor, Faculty of Engineering Mechanics Electrics and Electronics, Guanajuato University, PhD in Pattern Recognition and Artificial Intelligence from Polytechnic University of Valencia, Spain. Contributor in research

projects in the area of electrical engineering, Pattern Recognition and Artificial Intelligence

Dr. J. Rosales-Garcia; holds his MSc in 1991 from Faculty of physics at Kharkov State University, Ukraine and PhD in 1997 from Universidad Autónoma Metropolitana-Iztapalapa, México. He worked as a postdoctoral researcher for two years in the Bogoliubov Laboratory of Theoretical Physics, JINR, Dubna, Russia. He joined the Department of electrical engineering of División de Ingenierías Campus Irapuato-Salamanca, Universidad de Guanajuato on March 2003. He has written more than 50 papers published in journals indexed in SCI. His current research focuses on application of fractional calculus in physics and engineering. Dr. Rosales is an active member of the National Researcher System.